Journal of Microbiology, Immunology and Infection 56 (2023) 464—476

Available online at www.sciencedirect.com

ScienceDirect

journal homepage: www.e-jmii.com

Original Article

Role of the stress-responsive two-component system CpxAR in regulating fimbriae expression in *Klebsiella pneumoniae* CG43

Chih-Hao Kuo [a,1], Wei-Feng Lin [b,1], Chia-Jui Liu [a], Zhe-Chong Wang [a], Ting-Yi Liu [b], Hwei-Ling Peng [a,b,*]

[a] *Department of Biological Science and Technology, School of Biological Science and Technology, National Yang Ming Chiao Tung University, Hsin Chu, Taiwan*
[b] *Institute of Molecular Medicine and Bioengineering, School of Biological Science and Technology, National Yang Ming Chiao Tung University, Hsin Chu, Taiwan*

Received 17 August 2022; received in revised form 6 February 2023; accepted 18 February 2023
Available online 25 February 2023

KEYWORDS
CpxAR two-component system;
Iron homeostasis control;
Klebsiella pneumoniae CG43;
Small RNA RyhB;
Type 3 fimbriae expression

Abstract *Background:* CpxAR is a two-component system that allows bacteria to reorganize envelope structures in response to extracellular stimuli. CpxAR negatively affects type 1 fimbriae expression in *Klebsiella pneumoniae* CG43, a hypervirulent strain. The involvement of CpxAR in the regulation of type 3 fimbriae expression was investigated.
Methods: *cpxAR*, *cpxA*, and *cpxR* gene-specific deletion mutants were generated. The deletion effects on the expression of type 1 and type 3 fimbriae were analyzed via measuring the promoter activity, mannose sensitive yeast agglutination activity, biofilm formation, and the production of the major pilins FimA and MrkA respectively. RNA sequencing analysis of CG43S3, Δ*cpxAR*, Δ*cpxR* and Δ*fur* was employed to study the regulatory mechanism influencing the expression of type 3 fimbriae.
Results: Deletion of *cpxAR* increased type 1 and type 3 fimbrial expression. Comparative transcriptomic analysis showed that the expression of oxidative stress-responsive enzymes, type 1 and type 3 fimbriae, and iron acquisition and homeostasis control systems were differentially affected by *cpxAR* or *cpxR* deletion. Subsequent analysis revealed that the small RNA RyhB negatively affects the expression of type 3 fimbriae, while CpxAR positively controls *ryhB* expression. Finally, the site-directed mutation of the predicted interacting sequences of RyhB with the mRNA of MrkA attenuated the RyhB repression of type 3 fimbriae.

* Corresponding author. Department of Biological Science and Technology, National Yang Ming Chiao Tung University, 75 Po Ai Street, Hsin Chu, 30068, Taiwan.
E-mail address: hlpeng@nycu.edu.tw (H.-L. Peng).
[1] Equal contribution.

https://doi.org/10.1016/j.jmii.2023.02.003

Conclusion: CpxAR negatively regulates the expression of type 3 fimbriae by modulating cellular iron levels thereafter activating the expression of RyhB. The activated RyhB represses the expression of type 3 fimbriae by base-pairing binding to the 5′region of *mrkA* mRNA.

Introduction

Klebsiella pneumoniae, which may cause pneumonia, urinary tract infections, bacteremia, meningitis, endophthalmitis, and pyogenic liver abscess, are newly grouped into classical and hypervirulent strains owing to their multidrug resistance and invasiveness, respectively.[1—3] *K. pneumoniae* CG43, a K2 serotype isolated from the liver abscess of a diabetic patient, is a hypervirulent strain.[1] The characterized virulence traits include the large virulence plasmid pLVPK,[4] activator for the biosynthesis of capsular polysaccharides (CPS) RmpA and RmpA2,[5] adherence factors type 1 and type 3 fimbriae,[6] and two-component systems (TCS).[7—11]

The stress response TCS CpxAR identified in all Enterobacteria and several other Gram-negative bacteria[12] contains the inner membrane sensor kinase CpxA and the cytoplasmic response regulator CpxR. Upon stress stimuli, CpxA autophosphorylates and transfers the phosphoryl group to CpxR, and the phosphorylated CpxR controls the expression of genes involved in envelope stress responses. Through phosphorylation by the non-discriminate phosphodonor acetyl phosphate, the active CpxR-P may still accumulate in the CpxA deficient bacteria which lacks the specific kinase and phosphatase activities.[13—15] The inhibition of the autokinase activity of CpxA by the binding of CpxP, an alkaline-induced periplasmic chaperone, is relieved by the competition of stress-induced misfolded proteins for interaction with CpxP[16,17] Besides stress-induced misfolded proteins in the periplasm such as defects in the assembly of the outermembrane protein (OMP) or overexpression of the misfolded pilin subunit, CpxAR is also activated by environmental stimuli including high osmotic strength, depletion of iron, alkaline pH, and antibiotics.[16—18] The CpxAR regulon includes genes involved in the biosynthesis of envelope structures, such as CPS,[16,17] extracellular polysaccharides (EPS),[16,17] and the assembly of OMP,[19] and those involved in the inner membrane-associated processes.[16,17] In addition, *Escherichia coli* Cpx system can impede adherence to epithelial cell surfaces by downregulating the expression of P and type IV pili.[20,21] CpxAR negatively and indirectly affects type 1 fimbriae activity via the PecSM system in *K. pneumoniae* CG43.[11]

In many enterobacteria, type 1 fimbriae, encoded by *fimAICDFGH* operon, play a critical role in establishing urinary tract infection.[6] Type 3 fimbriae, encoded by *mrkABCDF* operon and commonly expressed in *K. pneumoniae*, mediate adherence to tracheal epithelial cells, renal tubular cells, and basolateral surfaces of lung tissue, and are also crucial for biofilm formation.[22] Their expression is positively regulated by the second messenger cyclic di-GMP (c-di-GMP) and MrkHI, and iron and Fur.[23]

This study reports the deletion effects of *cpxAR* in *K. pneumoniae* CG43, and RNA sequencing analysis was used to identify the components involved in the CpxAR regulatory network. The mechanism by which CpxAR regulates the expression of type 3 fimbriae was investigated.

Methods

Bacteria, plasmids, primers, and cultured condition

The bacterial strains and plasmids, and the primers used or constructed in this study are listed respectively in Tables 1 and 2. Bacterial strains were grown at 37 °C in Luria-Bertani (LB) broth (tryptone-10 g, yeast extract-5 g and NaCl-10 g/1 L, Cyrusbioscience, Taiwan) with antibiotics including ampicillin (100 μg/ml), chloramphenicol (35 μg/ml), kanamycin (25 μg/ml), or streptomycin (500 μg/ml).

Construction of the gene deletion mutants

The mutants Δ*cpxA* and Δ*cpxR* were constructed by using an allelic-exchange strategy. Briefly, 1-kb DNA fragment flanking both ends of *cpxA* or *cpxR* gene were PCR amplified with the respective primer pairs (Table 2) and then the amplicons individually cloned into pKAS46.[24] The resulting plasmid was firstly transformed into *E. coli* S17-1 λ*pir* and then mobilized by conjugation into *K. pneumoniae* CG43S3. The specific gene deletion mutants were screened and isolated accordingly as described.[11]

Assessment of type 1 and type 3 fimbriae expression

Expression of type 1 fimbriae was determined by analysis of *fimA*, *fimB*, and *fimE* promoter activity, the major pilin FimA production, and mannose sensitive yeast agglutination as described.[11] Type 3 fimbriae expression was recorded by measuring *mrkA* and *mrkH* promoter activity, the major pilin MrkA production, and biofilm formation described previously.[23] Briefly, the promoter reporter plasmids were individually introducing into *K. pneumoniae* strains by electroporation or conjugation from *E. coli* S17-1λ *pir*, and each of the β-galactosidase activity measured. The relative biofilm formation levels were determined by crystal violet staining, and the stained biomass solubilized in 1% (w/v) SDS and absorbance at 600 nm measured.

Statistical analyses

The data of biofilm formation and promoter activity were derived from a single experiment which is representative of three independent assays. Each sample was assayed in

Table 1 Bacteria and plasmids used in the study.

strain or plasmid	properties	reference or source
E. coli		
S17-1 λ*pir*	RecA *thi pro hsdR*$^{-}$M+ [RP4-2-Tc::Mu:KmRTn*7*]	Laboratory stock
K. pneumoniae		
CG43	clinical isolate of K2 serotype	Laboratory stock
CG43S3	*rspL* mutant, Sm^{r}	Laboratory stock
Δ*lacZ*	*lacZ* gene removed from CG43S3	[11]
Δ*mrkA*	*mrkA* gene removed from CG43S3	[23]
Δ*fimA*	*fimA* gene removed from CG43S3	Laboratory stock
Δ*cpxAR*	*cpxA* and *cpxR* genes removed from CG43S3	[11]
Δ*cpxA*	*cpxA* gene removed from CG43S3	This study
Δ*cpxR*	*cpxR* gene removed from CG43S3	This study
Δ*cpxAR*::*cpxAR*	CG43S3Δ*cpxAR* complemented with *cpxA* and *cpxR* genes in genome	[11]
Δ*lacZ*Δ*cpxAR*	*lacZ* genes removed from Δ*cpxAR*	[11]
Δ*fur*	*fur* gene removed from CG43S3	[25]
Δ*ryhB*	*ryhB* gene removed from CG43S3	[25]
Δ*fur*Δ*ryhB*	*ryhB* gene removed from Δ*fur*	[25]
Δ*cpxAR*Δ*fur*	*cpxAR* gene removed from Δ*fur*	This study
Δ*cpxAR*Δ*fur*Δ*ryhB*	*cpxAR* gene removed from Δ*ryhB*Δ*fur*	This study
Δ*cpxAR*Δ*ryhB*	*cpxAR* gene removed from Δ*cpxAR*Δ*ryhB*	This study
plasmid		
yT&A	PCR cloning vector, Ap^{r}	Laboratory stock
pKAS46	suicide vector, *rpsL*, Km^{r}, Ap^{r}	[24]
pKAS46-cpxAR	Km^{r} and Ap^{r}, suicide vector for *cpxAR* deletion	This study
pKAS46-cpxA	Km^{r} and Ap^{r}, suicide vector for *cpxA* deletion	This study
pKAS46-cpxR	Km^{r} and Ap^{r}, suicide vector for *cpxR* deletion	This study
pLacZ15	containing the promoterless lacZ from *K. pneumoniae* CG43S3, Cm^{r}	[7]
pP_{fimA}-lacZ	pLacZ15 harboring the putative promoter of *fimA*	[39]
pP_{fimB}-lacZ	pLacZ15 harboring the putative promoter of *fimB*	[39]
pP_{fimE}-lacZ	pLacZ15 harboring the putative promoter of *fimE*	[39]
pP_{mrkA}-lacZ	pLacZ15 harboring the putative promoter of *mrkA*	[23]
pP_{mrkH}-lacZ	pLacZ15 harboring the putative promoter of *mrkH*	[23]
pP_{ryhB}-lacZ	pLacZ15 harboring the putative promoter of *ryhB*	[25]
pP_{fur}-lacZ	pLacZ15 harboring the putative promoter of *fur*	Laboratory stock
pP_{cpxP}-lacZ	pLacZ15 harboring the putative promoter of *cpxP*	This study
pQE81L-Kan	Km^{r}, expression vector	Laboratory stock
pQE81L -*cpxR*	Km^{r}, *cpxR* coding region cloned into pQE81L-Kan	[11]
pETQ-*ryhB*	Km^{r}, pETQ plasmid containing 326-bp fragment of the promoter and coding region of *ryhB*	[25]
pETQ-$ryhB_{2\text{-}14}$	Km^{r}, pETQ plasmid containing 326-bp fragment of the promoter and coding region of *ryhB* with the mutated sequences from nucleotides 2 to 14	This study
pETQ-$ryhB_{11\text{-}14}$	Km^{r}, pETQ plasmid containing 326-bp fragment of the promoter and coding region of *ryhB* with the mutated sequences from nucleotides 11 to 14	This study

Cm^{r}, chloramphenicol resistance; Sm^{r}, streptomycin resistance; Km^{r}, kanamycin resistance.

triplicate and the activity and standard deviations were presented. Two independent sample Student t-test were used and P value less than 0.05 was considered statistically significant, and all tests were two-tailed. The statistical significance was set to $^{*}p < 0.05$, $^{**}p < 0.01$ and $^{***}p < 0.001$.

RNA sequencing analysis

Total RNAs were isolated from CG43S3, Δ*cpxAR*, Δ*cpxR* and Δ*fur* using RNeasy MinElute Cleanup Kit (Qiagen). The RNAs were sequenced with the assigned number NM14120006 using Illumina's sequencing instrument by TRI-I BIOTECH INC (New Taipei City, Taiwan). FASTX-Tool was applied to remove or trim deep sequencing reads with low quality bases and the adaptor sequences. The remaining reads were mapped to *K. pneumoniae* CG43 genome for the expression levels estimation (NCBI Taxonomy ID: 1244085) using CLC Genomics Workbench v10. The genes with log 2-fold change greater than 2 (up and down) as compared with those of Δ*cpxAR* or Δ*cpxR* were identified as significantly transcript abundance changed in CG43S3. Finally, the annotation tools, DAVID, was used to illustrate the biological regulation role from Gene Ontology (GO) or Kyoto Encyclopedia of Genes and Genomes (KEGG).

Table 2 Primer used in this study.

primer	sequence (5'→3')	
For specific gene-deletion mutants		Target
cpxA-AF	GAATTCCTGTAGCAAGGAGAGCAGCCATG	*cpxA*
cpxA-AR	GGTACCTATTCAGCAGCACCGCGGC	
cpxA-BF	GGTACCTCCAGCAGCTCGGTCATCTG	
cpxA-BR	TCTAGAGCGGGCCTTGATGACGTAAT	
WCC174	AATTCTAGACGCAGCAGGGCGGTACCCAATTGCA	*cpxR*
WCC175	AATAGATCTAAAACGCTGCGTGGCCGCGGGTATC	
WCC140	AGATCTTAAATCAACGCTGTCGTCCAGAAG	
WCC141	GAATTCGTTTGTTACTGGGGTTGCAGG	
For protein expression		
WCC148	GGATCCGATGAATAAAATCCTGTTAGTTGATGAT	CpxR
WCC149	AAGCTTCATGAAGCGGAAACCATCAGATAC	
For RNA expression		
ryhB mut1F	GGCTTTCCGCTTCCGTCTCCCTGAATGCAGG	*ryhB*
ryhB mut1R	GAGACGGAAGCGGAAAGCCTGAAAGCACGACATTG	
EMSA		
wcc176	GGATCCGGCGCAGAATCGCGCGTATA	*cpxP*
wcc177	ACATCTCATGACGGCAGCGATAACATTGCG	
pcc323	GGATCCTGCATGCTGTTGCGGTCAC	*mrkA*
pcc324	GGATCCGCGGTTGCCATTGCTGCAGAG	
wcc54	GAACTTATATTTTTAGGTTCGTTACCTGACGCC	*mrkA*-T
GT44	GGATCCGCAAGGGTCTCCCTG	*ryhB*
GT45	AGATCTCGGTTCAGCATGGCGTATC	
ryhB-T-R	GGCGG CCGGG GAGTC AAT	*ryhB*-T

DNA electrophoretic mobility shift assay (EMSA)

EMSA was performed as described[11] with some modifications. Breifly, the putative promoter region of *cpxP*, *mrkA*, *mrkA*-T, *rhyB* and *rhyB*-T were PCR-amplified using the respective primer pairs (Table 2). Each of the PCR product (100 ng) was mixed with increasing concentrations from 15 to 30 nM of His_6-CpxR in a 20 μL binding buffer (20 mM pH 7.0 Tris-HCl, 30 mM acetyl phosphate, 125 mM KCl, 10 mM $MgCl_2$, 1 mM EDTA, 1 mM dithiothreitol, 0.25 mg/ml BSA), and the reaction mixture stood at room temperature for 30 min. The mixture was subsequently resolved on 5% native polyacrylamide gel by electrophoresis and the DNA bands were stained using SYBR.

Generation of pETQ-*ryhB*$_{2\text{-}14}$ and pETQ-*ryhB*$_{11\text{-}14}$

The 326-bp DNA, *ryhB*$_{2\text{-}14}$, containing promoter and the mutated coding region of RyhB (the nucleotides from 2 to 14 substituted with their complementary sequences) was synthesized and cloned in to plasmid pEZClone-NRS-Blunt-HC (APOLO Biochemical, Inc.). The *ryhB*$_{2\text{-}14}$ DNA was then isolated from the recombinant pEZ-*ryhB*$_{2\text{-}14}$ and subcloned into plasmid pETQ[25] using *Bam*HI and *Hin*dIII digestion. On the other hand, the recombinant plasmid pETQ-*ryhB*$_{11\text{-}14}$ was generated using inverse PCR. Briefly, PCR reaction was carried out with Pfu Ultra II Fusion HS DNA polymerase (Agilent Technologies) using the primer pairs, *ryhB* mut1F and *ryhB*mut1R, containing the altered sequences from nucleotide 11 to 14 of *ryhB*, and pETQ-*ryhB*[25] as template. The PCR product was then subjected to *Dpn*I digestion, T4 polynucleotide kinase treatment and self-ligation. Finally, the ligation product was transformed into *E. coli* JM109 and the resulting plasmid pETQ-*ryhB*$_{11\text{-}14}$ was confirmed using sequencing analysis.

Results

CpxAR negatively controls the expression of type 1 and type 3 fimbriae

Considering that a negative role has been reported for CpxAR in type 1 fimbriae expression in *K. pneumoniae* CG43,[11] the effect of *cpxAR* deletion on the expression of type 3 fimbriae was investigated. Fig. 1A showed deletion of *cpxAR* increased the production of the major pilin of type 3 fimbriae MrkA as well as that of type 1 fimbriae FimA. Complementation analysis by integration *cpxAR* gene to Δ*cpxAR* supported a negative control of CpxAR on the production of FimA and MrkA. Deletion of *cpxAR* from CG43S3 increased mannose-sensitive yeast agglutination activity (Fig. 1B), but reduced biofilm formation (Fig. 1C).

As shown in Fig. 2A, several sequences homologous to the CpxR-binding elements -GTAAA $N_{5\text{-}8}$ GTAAA-[16] were identified in the putative promoter regions of *fimA*, *fimB*, *fimE*, *mrkA*, and *mrkH*. Thus, the β-galactosidase activities of P_{fimA}, P_{fimB}, P_{mrkA}, and P_{mrkH} were measured in Δ*cpxAR* and compared with those in CG43S3. The upper panel of Fig. 2A indicated that the activities of P_{fimA}, P_{fimB}, and P_{mrkA} were increased by the deletion of *cpxAR*, suggesting a negative role of CpxAR in the expression of types 1 and 3 fimbriae at the transcriptional level. In addition, the EMSA

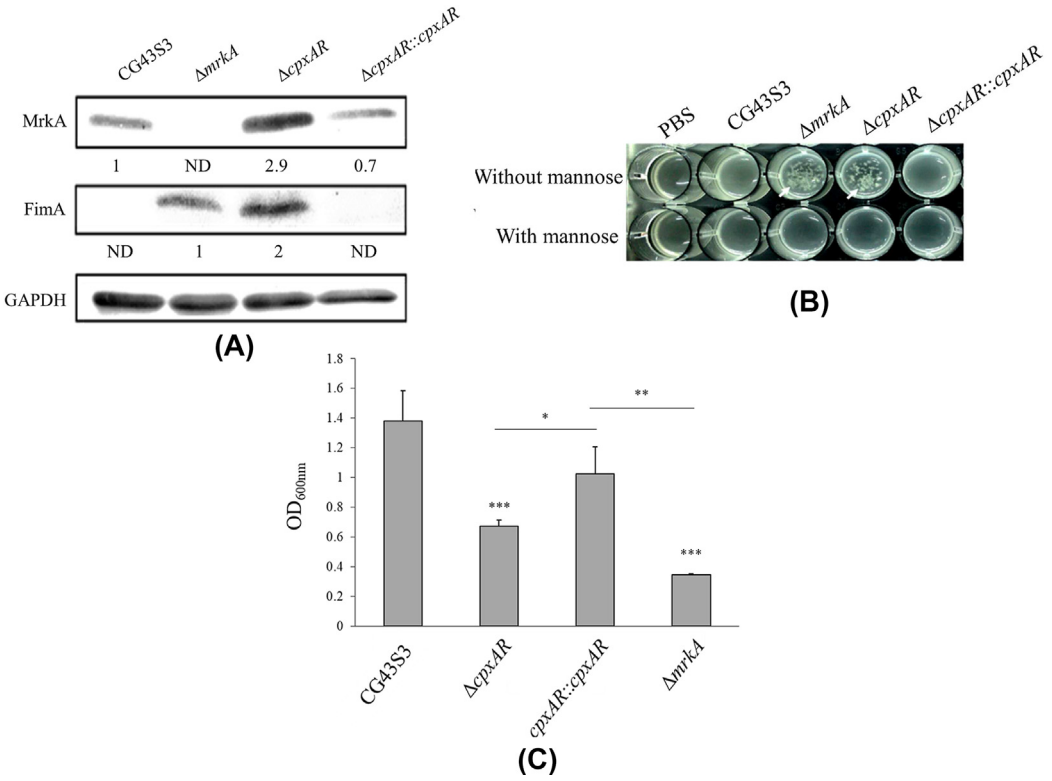

Figure 1. Influence of *cpxAR* deletion on the expression of type 1 and type 3 fimbriae. Type 1 and type 3 fimbriae expression determined using western blotting against anti-FimA and anti-MrkA antibody(A), mannose-sensitive yeast agglutination assay (B), and biofilm formation (C). The bacteria Δ*mrkA* and Δ*fimA* were used as negative control for MrkA and FimA expression, respectively. The amount changes of MrkA and FimA calculated using ImageJ software and GAPDH was a protein loading control. The statistical labels indicated that the biofilm formation was significantly different from that of CG43S3 unless otherwise marked by lines.

analysis in Fig. 2B showed that the purified His_6-CpxR (sFig. 1) of 15- or 30-nM was able to form binding complexes with the probe DNA of *cpxP* or *mrkA* but not *mrk-T* that removed of the putative CpxR box. This suggests a direct regulation of CpxR on *mrkA* expression.

The CpxAR-dependent expression genes identified by RNA sequencing analysis

The comparative analysis of RNA sequencing data of CG43S3, Δ*cpxAR*, and Δ*cpxR* were collected. As shown in Table 3, those with twofold changes in their transcriptional levels were selected and classified into seven functional groups. *cpxP* expression was significantly reduced by removing *cpxAR* or *cpxR* genes, and *cpxA* expression after deletion of the *cpxR* gene, both corroborating the reliability of the analysis. Collectively, transcription of the signal transduction genes *rcsA*, *zraS*, *rstB*, and *yfiN*; the membrane protein genes *ompF*, *ompA* and *ompW*; and the stress response genes *groES*, *sodA*, *dnaK*, and *katE* was found to be differentially affected. The transcript levels of the genes *glpQ*, *glpT*, *glpD*, and *glpK* required for glycerol metabolism were decreased by either *cpxAR* or *cpxR* gene deletion, whereas those of *nirD*, *narX*, *narZ*, and *narK* for nitrite metabolism were decreased by *cpxR* deletion. The expression of the genes involved in iron acquisition, storage, and homeostatic control systems was differently influenced. Specifically, the expression levels of *foxA*, *entE*, *entC*, *fur*, and *cirA* were decreased by the deletion of *cpxAR* or *cpxR*. The expression level of the iron transporter *feoB* was decreased, while those of IscR and SufC were increased by *cpxAR* deletion. Moreover, the transcript levels of *mrkA*, *mrkH* and *fimA* were increased after removing *cpxAR* gene, which supporting the findings in Fig. 2A that CpxAR negatively regulated the expression of *mrkA* and *fimA* at the transcriptional levels.

The phosphorylated CpxR exerts no regulatory effect on MrkA production

RNA sequencing analysis revealed that *fimA* transcription was significantly enhanced only by the deletion of *cpxAR*, but not *cpxR*. In contrast, the deletion of *cpxAR* or *cpxR* increased the *mrkA* and *mrkH* transcript levels (Table 3). This implies a different control of the phosphorylated form of CpxR on the expression of types 1 and 3 fimbriae. As reported in *E. coli*,[13] *Yersinia pseudotuberculosis*,[14] and *Salmonella enterica* serovar Typhimurium,[15] the bacteria deficient in CpxA may acquire the phosphoryl group from the metabolic by-product acetyl phosphate to render its CpxR in a constitutively phosphorylated form. We then generated a *cpxA* deletion mutant and compared the

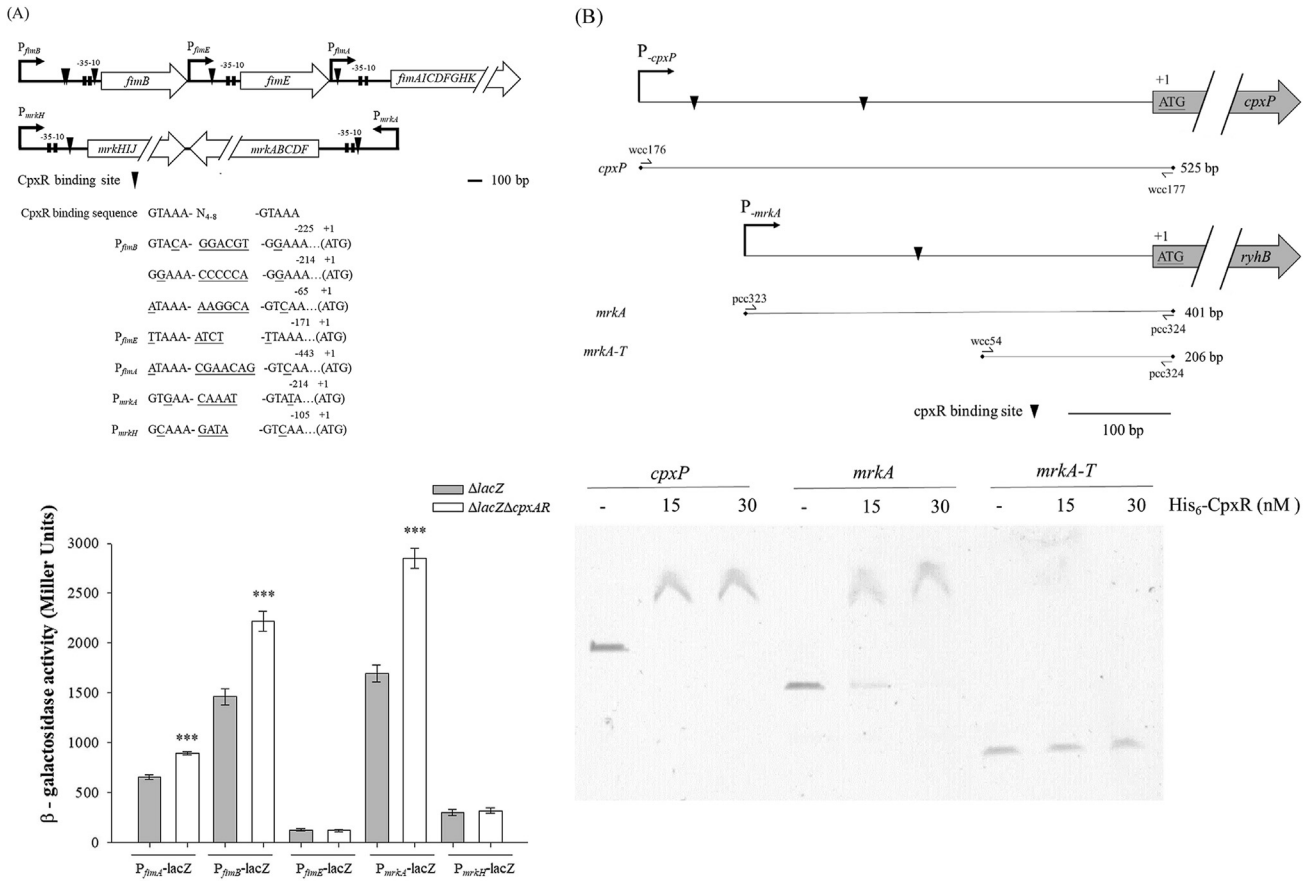

Figure 2. Analysis of CpxAR regulation on the expression of type 1 and type 3 fimbriae. (A) The consensus CpxR box on the putative promoter region is marked on the upper panel and the β-galactosidase activities were determined below. The statistical labels indicated that the promoter activity was significantly different from that of Δ*lacZ*. (B) EMSA of the interaction between the recombinant CpxR protein and the probe DNA of *cpxP*, *mrkA* or *mrkA-T*. Schematic presentation of the size and relative location of the probe *cpxP* (as the positive control), *mrkA* or *mrkA-T* (removed of the putative CpxR box) is shown above.

expression of type 1 and type 3 fimbriae with those of CG43S3, Δ*cpxAR*, and Δ*cpxR*. As shown in Fig. 3, the *cpxA* deletion significantly increased FimA production but slightly decreased MrkA production compared with those of CG43S3. This suggests that the negative regulation of CpxAR of type 3 fimbriae is different from that of type 1 fimbriae which is dependent on the phosphorylation control of CpxR. The underlying mechanism for the differential control remains to be investigated.

CpxAR positively affects the expression of the iron homeostasis regulator RyhB

RNA sequencing analysis in Table 3 suggests that the CpxAR-dependent expression of type 3 fimbriae may be determined by controlling the iron levels. The expression of type 3 fimbriae is positively regulated by iron and Fur.[23] The small RNA RyhB as well as Fur is the major regulator for modulating the iron levels in *K. pneumoniae*,[25] *Vibrio cholera*,[26] *E. coli*,[27] and *Salmonella* Typhimurium.[28] As shown in Fig. 4A, a consensus CpxR-binding box was identified in the putative promoter region of *fur* and *ryhB*, suggesting that transcription of *ryhB* is also regulated by the CpxAR system. To examine this possibility, we measured and compared the promoter activities of CG43S3 and Δ*cpxAR*. Although deletion of *cpxAR* had no apparent effect on *fur* expression, the promoter activities of *ryhB* as well as *cpxP* were significantly reduced (Fig. 4A), suggesting a positive role of CpxAR in the expression of *ryhB*, but not *fur*. Deletion of *cpxAR* or *cpxR* had no apparent effect on the production of Fur, supporting the possibility (Fig. 4B). As shown in Fig. 4C, the recombinant CpxR of 15 nM was able to form binding complex with *cpxP* while the binding complex of CpxR-*ryhB* was only observed with 30 nM CpxR, implying that the CpxR exhibiting less binding affinity to *ryhB* than *cpxP*. In order to assess the binding specificity of CpxR, *mrk*-T of which carrying similar size as the *ryhB* probe and exhibiting no binding activity to CpxR was used as the negative control. No binding complex of 30 nM CpxR with *mrkA-T* or *ryhB-T*, the truncated probe without CpxR box, was observed suggesting a positive and direct regulation of CpxR on the expression of *ryhB* at the transcriptional level.

CpxAR repression of type 3 fimbriae expression is mediated by RyhB

As shown in Table 4, the expression of RyhB is significantly increased by the deletion of *fur* gene. This is consistent with

Table 3 Expression of the genes influenced by deletion of *cpxAR* or *cpxR*.

Gene name	Δ*cpxAR*/ CG43S3	Δ*cpxR*/ CG43S3	Proposed function
Signal transduction			
cpxP	−6.52	−25.4	CpxA periplasmic repressor
cpxA	-	−2.52	2CS sensor protein
rcsA	-	−2.67	2CS response regulator
zraS	−3.35	-	2CS sensor protein
rstB	2.14	-	2CS response regulator
yfiN	2.01	-	diguanylate cyclase
Stress response			
groEL	2.83	−2.66	chaperonin
sodA	-	−3.09	superoxide dismutase
sodB	-	2.08	superoxide dismutase
dnaK	2.15	-	molecular chaperone
groES	2.09	-	molecular chaperone
katE	2.39	-	catalase II
Outer membrane protein			
ompF	3.57	-	outer membrane protein F
ompA	-	−2.55	outer membrane protein A
ompW	-	3.09	outer membrane protein W
Glycerol metabolism			
glpQ	−5.35	−6.74	glycerophosphodiester phosphodiesterase
glpT	−3.73	−10.08	sn-glycerol-3-phosphate transporter
glpD	−2.71	−5.46	glycerol-3-phosphate dehydrogenase
glpK	−2.07	−3.75	glycerol kinase
glpC	3.12	-	glycerol-3-phosphate dehydrogenase subunit C
Nitrate metabolism			
nirD	-	−5.15	nitrite reductase small subunit
narX	-	−4.16	nitrate/nitrite sensor protein
narZ_2	-	−2.9	nitrate reductase A subunit alpha
nark	-	−2.83	nitrate/nitrite transporter
Iron acquisition and homeostasis			
foxA	−5.76	−4.78	ferrichrome-iron receptor
entE	−4.55	−4.57	enterobactin synthase subunit E
entC	−3.57	−5.6	isochorismate synthase
feoB	−3.07	-	iron transporter
fur	-	−2.06	ferric uptake regulator
cirA	-	−2.06	catecholate siderophore receptor
iscR	3.67	2.01	Fe−S cluster assembly transcriptional regulator
sufC	2.13	-	Fe−S cluster assembly ATPase
Fimbriae expression			
mrkH	9.48	5.62	PilZ domain protein
mrkA	6.08	5.14	Type 3 fimbriae subunit A
fimA	5.24	-	Type 1 fimbriae subunit A

The gene expression ratio of mutant relative to the parental strain CG43S3 with a fold change ≥2 was recorded while '-' used to mark those not reached the fold change levels.

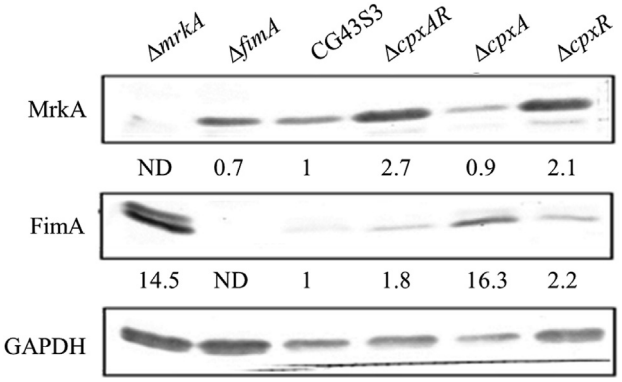

Figure 3. Differential regulation of the phosphorylated CpxR on the expression of MrkA and FimA. The effect of the phosphorylation status of CpxR was determined by comparing the production of FimA and MrkA, assessed using western blotting analysis against anti-FimA and anti-MrkA antibody respectively, in Δ*cpxA*, which carrying a constitutively phosphorylated form of CpxR, with those in CG43S3, Δ*cpxAR*, and Δ*cpxR*.

the findings observed in *E. coli*, where the expression of *ryhB* is directly repressed by Fur.[29] As the expression of *mrkA*, *mrkH*, and *mrkI* was decreased in Δ*fur* (Table 4), the involvement of RyhB in the Fur-dependent expression of type 3 fimbriae was investigated. Fig. 5A and B showed the deletion of *fur* from CG43S3 inhibited MrkA production and biofilm formation, while removing *ryhB* gene from Δ*fur* restored MrkA production and biofilm formation to levels comparable to those of CG43S3. In the absence of *fur*, RyhB is active and the expression of type 3 fimbriae is inhibited, whereas the repression is released by removing *ryhB* gene from Δ*fur*.

To further investigate the involvement of RyhB in CpxAR repression of type 3 fimbriae, comparative analysis of MrkA production in CG43S3, Δ*cpxAR*, Δ*fur*, Δ*cpxAR*Δ*fur*, and Δ*cpxAR*Δ*fur*Δ*ryhB* showed approximately threefold increase by deleting *cpxAR* and decrease to undetectable levels in Δ*fur* (Fig. 5C), supporting the negative role of CpxAR and RyhB on MrkA expression. Comparison of Δ*cpxAR*, Δ*cpxAR*Δ*fur*, and Δ*cpxAR*Δ*fur*Δ*ryhB* revealed that MrkA production and biofilm formation levels of Δ*cpxAR* were reduced by removing *fur* gene, but restored by further deletion of the *ryhB* gene from Δ*cpxAR*Δ*fur*, indicating that CpxAR repression of type 3 fimbriae expression was mediated by RyhB (Fig. 5D).

RyhB directly affects the expression of type 3 fimbriae by base-pairing with the mRNA of MrkA

Fig. 6A showed the β-galactosidase activity of CG43S3, which was lowered by deleting *fur* gene, was restored by further removing *ryhB*, indicating a negative role of RyhB in the expression of *mrk* operon. RyhB repression of target genes occurs via an antisense mechanism by base-pairing with the mRNA in the translation initiation region.[29] Sequence analysis using intaRNA software was then

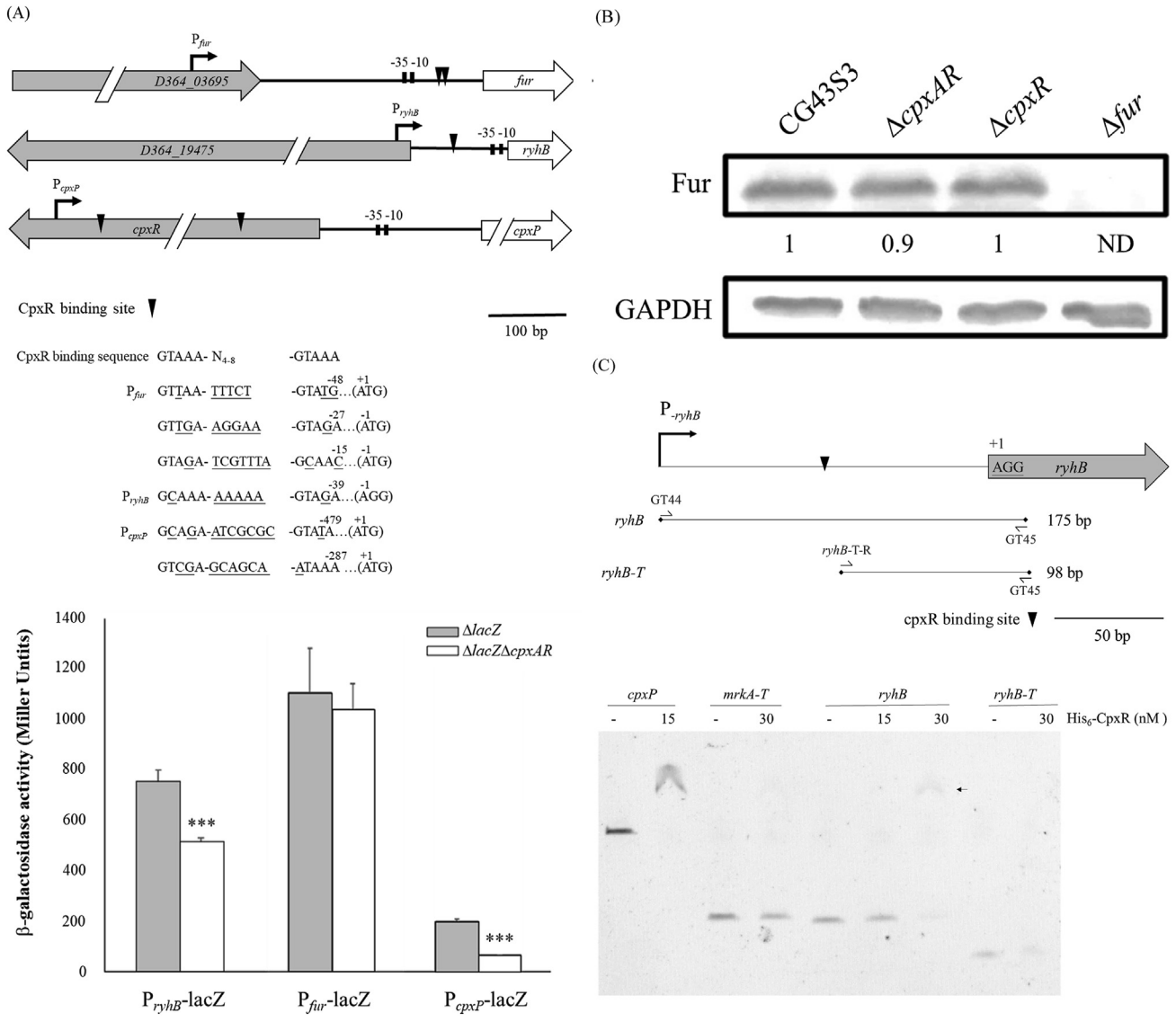

Figure 4. Analysis of CpxAR regulation on the expression of *fur* and RyhB. (A) The consensus CpxR box on the putative promoter region is marked on the upper panel and the β-galactosidase activities influenced by *cpxAR* deletion were determined below. The statistical labels indicated that the promoter activity measured in Δ*lacZ*Δ*cpxAR* was significantly lower than that in Δ*lacZ*. (B) Western blot analysis for the *cpxAR* deletion on Fur production assessed using anti-Fur antibody. (C) EMSA of the interaction between the recombinant CpxR protein and the promoter of *cpxP*, *mrkA*-T *ryhB* and *ryhB*-T. The probe cpxP was the positive control while *mrkA*-T the negative control for the binding analysis. The upper panel schematically shows the size and relative location of the probe *ryhB* and *ryhB*-T without the putative CpxR box. The arrow marks the binding complex of CpxR-*ryhB*.

performed to determine the possible RyhB binding region on mRNA *mrkA*. Fig. 6B showed the predicted interaction site was located at the 5′-end coding region of *mrkA*, which is capable of forming two base-pairing forms with the RyhB sequence from nucleotides 2 to 14. Recombinant pETQ-$ryhB_{2\text{-}14}$ (containing the complementary sequences from nucleotides 2 to 14 of *ryhB*) and $RyhB_{11\text{-}14}$ (containing the complementary sequences from nucleotides 11 to 14 of *RyhB*) were generated (Fig. 6B). As shown in Fig. 6C, MrkA production was blocked when CG43S3 was transformed with pETQ-*ryhB*, but not with the mutated form $ryhB_{2\text{-}14}$ or $ryhB_{11\text{-}14}$. The comparison of biofilm formation in Fig. 6D among CG43S3[pETQ], CG43S3[pETQ-*ryhB*], CG43S3[pETQ-$ryhB_{2\text{-}14}$], and CG43S3[pETQ-$ryhB_{11\text{-}14}$] also revealed a similar trend to that shown in Fig. 6C, in which nucleotides 2—14 of RyhB played a critical role in negative regulation. These results suggest that RyhB directly binds to the mRNA of *mrkA* in an antisense manner to negatively regulate the expression of type 3 fimbriae.

Discussion

Deletion of *cpxAR* from *K. pneumoniae* CG43S3 significantly decreased its resistance to different antibiotics (Fig. S2A) and stress reagents, including H_2O_2, paraquat, SDS, and bile

Table 4 Expression of the genes influenced by deletion of *fur*.

Gene name	Δ*fur*/CG43S3	Gene description
sRNA		
ryhB	60.4	involved in iron metabolism
Iron homeostasis		
fhuA	23.7	ferrichrome outer membrane transporter
feoA	8.2	iron transporter
feoB	6.7	iron transporter
entF	114.9	enterobactin synthase subunit F
entE	983.9	enterobactin synthase subunit E
D364_02680	10.2	iron-siderophore ABC transporter permease
D364_03165	137.8	enterobactin/ferric enterobactin esterase
D364_03180	97.8	iron-enterobactin transporter ATP-binding
D364_03185	61.0	iron-enterobactin transporter permease
D364_03190	175.0	iron-enterobactin transporter membrane protein
D364_03195	248.5	enterobactin exporter EntS
D364_05430	171.7	iron permease
D364_05435	51.8	iron ABC transporter substrate-binding protein
D364_10785	51.2	iron-enterobactin transporter ATP-binding protein
D364_17130	27.2	hemolysin
D364_10775	18.6	iron ABC transporter
D364_02675	13.9	iron ABC transporter ATP-binding protein
D364_09095	5.7	hemolysin D
D364_15750	335.1	iron ABC transporter
D364_19340	7.1	iron transporter
D364_24600	34.8	ferric iron reductase involved in ferric hydroximate transport
Fimbriae		
mrkH	−2.6	PilZ domain protein
mrkI	−3.5	LuxR family transcriptional regulator
mrkA	−6.4	Type 3 fimbrial major subunit A
fimA	33.2	Type 1 fimbrial major subunit A

The gene expression ratio of mutant relative to the parental strain CG43S3 with a fold change ≥2 was recorded.

salts (Fig. S2B), as well as the production of OmpC (Fig. S3A). The *cpxAR* deletion defects were complemented by integrating *cpxAR*-containing DNA into Δ*cpxAR*, indicating a positive regulatory role of CpxAR in response to these stresses. These results are consistent with the Cpx system positively regulating the expression of efflux pumps and OmpC for multidrug resistance and stress tolerance in *K. pneumoniae* NTUH-K2044.[30,31]

Fig. S3(B) showed that *cpxAR* deletion significantly reduced CPS production. RNA sequencing analysis showed that the expression of *rcsA*, which encodes an activator for CPS biosynthesis,[32] was reduced by *cpxR* deletion (Table 3). This suggests that the positive regulation of CPS production by CpxAR is mediated by RcsA. It has been reported that CPS as well as type 3 fimbriae is a determinant for *K. pneumoniae* biofilm formation.[33] The reduction of biofilm formation by removing *cpxAR* genes (Fig. 1C) implies that CPS plays more important role than type 3 fimbriae in *K. pneumoniae* biofilm formation.

CpxR directly represses the expression of the GlpT transporter for glycerol-3-phosphate[34] in *E. coli* O157. In contrast, deletion of *cpxAR* or *cpxR* significantly reduced the expression of the genes involved in glycerol and nitrate metabolism (Table 3) in *K. pneumoniae*, suggesting a positive role for CpxAR in their regulation. The differential control of CpxAR on the glycerol metabolism between the two bacteria remains to be investigated.

In *E. coli*, Fur and RyhB are major regulators of iron homeostasis. Under iron-replete conditions, Fur, an iron-dependent negative regulator, complexes with ferrous ions to block the transcription of iron-acquisition genes and *ryhB*. With low iron levels, Fur becomes inactive thus releasing its negative control of RyhB. The active RyhB downregulates mRNA levels of iron-utilizing proteins by destabilizing their structure and promoting their degradation but increases the expression of those genes participating in elevating the intracellular iron levels.[29] As shown in Table 4, deletion of *fur* gene from *K. pneumoniae* also activated RyhB expression which leading to increase of the expression of the genes involved in iron uptake and transport systems.

As shown in Fig. 4A and C, promoter activity analysis revealed that the deletion of *cpxAR* significantly decreased the expression of RyhB, and a direct interaction of the phosphorylated form of the recombinant CpxR and the promoter of RyhB was demonstrated. It has been reported that *Vibrio cholera* CpxAR is induced under iron-limiting conditions to activate the iron acquisition systems.[18] We speculate that similarly under low iron levels *K. pneumoniae* CpxAR activates the expression of RyhB and the active

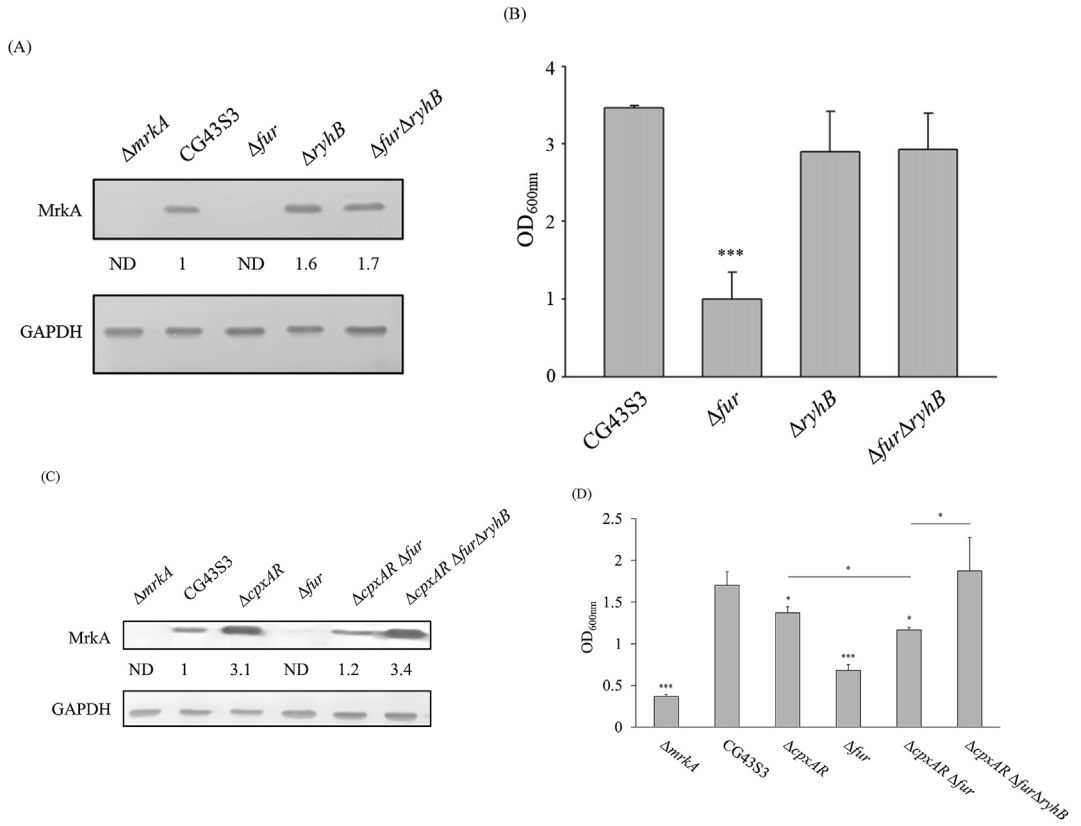

Figure 5. Analysis of CpxAR-RyhB regulation on the expression of type 3 fimbriae. Effects of *ryhB* or *fur* gene deletion, or *fur* and *ryhB* double deletion on the production of MrkA (A) and biofilm formation (B). Effects of *cpxAR*, *fur*, *cpxAR* and *fur* double deletion, or *cpxAR*, *fur*, and *ryhB* triple deletion on the production of MrkA (C) and biofilm formation (D) were analyzed. The statistical labels indicated that the biofilm formation was significantly different from that of CG43S3 unless otherwise marked by lines.

RyhB in turn downregulates the mRNA levels of iron-utilizing proteins. The differential deletion effects of *cpxAR* on the iron acquisition and storage systems is mediated by Fur and RyhB.

Besides controlling iron homeostasis, RyhB also regulates the virulence of *V. cholerae*[35] and *Shigella dysenteriae*.[36] Fig. 5A and B shows that in the absence of *fur*, MrkA production and biofilm formation were significantly reduced, and further removal of the *ryhB* gene from Δ*fur* could restore the wild-type levels. This finding demonstrates that the positive effect of Fur on the expression of type 3 fimbriae is mediated by RyhB. As shown in Fig. 5C, MrkA production by Δ*cpxAR* was reduced by removing the *fur* gene, but restored by further deletion of the *ryhB* gene from Δ*cpxAR*Δ*fur*. This again demonstrates that CpxAR plays a positive role in the expression of RyhB and that CpxAR repression of type 3 fimbriae is mediated by RyhB.

The expression of *ryhB*, but not the mutated form $RyhB_{2\text{-}14}$ or $RyhB_{11\text{-}14}$, blocked MrkA production and reduced biofilm formation, demonstrating a critical role of nucleotides 2—14 of RyhB in regulating the expression of type 3 fimbriae. Nevertheless, as Fur-dependent type 3 fimbriae expression is via a direct activation of MrkHI,[23] the involvement of MrkHI in the RyhB repression of type 3 fimbriae remains to be investigated.

Beside a post-translational level regulation of the assembly of P pilus and type IV pilus,[20,21] *E. coli* CpxAR also exerts a transcriptional level control of the expression of P pilus. Under environmental stress or alkaline growth conditions, competitively binding of the phosphorylated CpxR to the phase variation *pap* promoter results in inhibition of the P pilus expression.[37] In *K. pneumoniae*, CpxAR plays a negative role in the urate-responsive expression of type 1 fimbriae at the transcriptional level.[11] Here, we have demonstrated again a negative role of *K. pneumoniae* CpxAR on the expression of type 3 fimbriae. The model for CpxAR dependent expression of type 3 fimbriae is shown in Fig. 7. Under low iron levels, the activated CpxAR modulates the cellular iron levels through inducing the expression of the iron acquisition system and iron homeostasis regulators Fur and RyhB. Under sufficient iron levels, Fur forms a complex with ferrous ions to activate the expression of *mrkHI*, thereby enhancing the expression of type 3 fimbriae. When cellular iron is lowered to a certain level, the small RNA RyhB, which is no longer repressed by Fur-Fe^{2+}, is activated and concurrently increased by CpxAR. In conclusion, active RyhB directly inhibits the expression of *mrkABCDF* operon that codes for the type 3 fimbriae biosynthesis system via base-pairing binding to the 5′ sequences of *mrkA* mRNA.

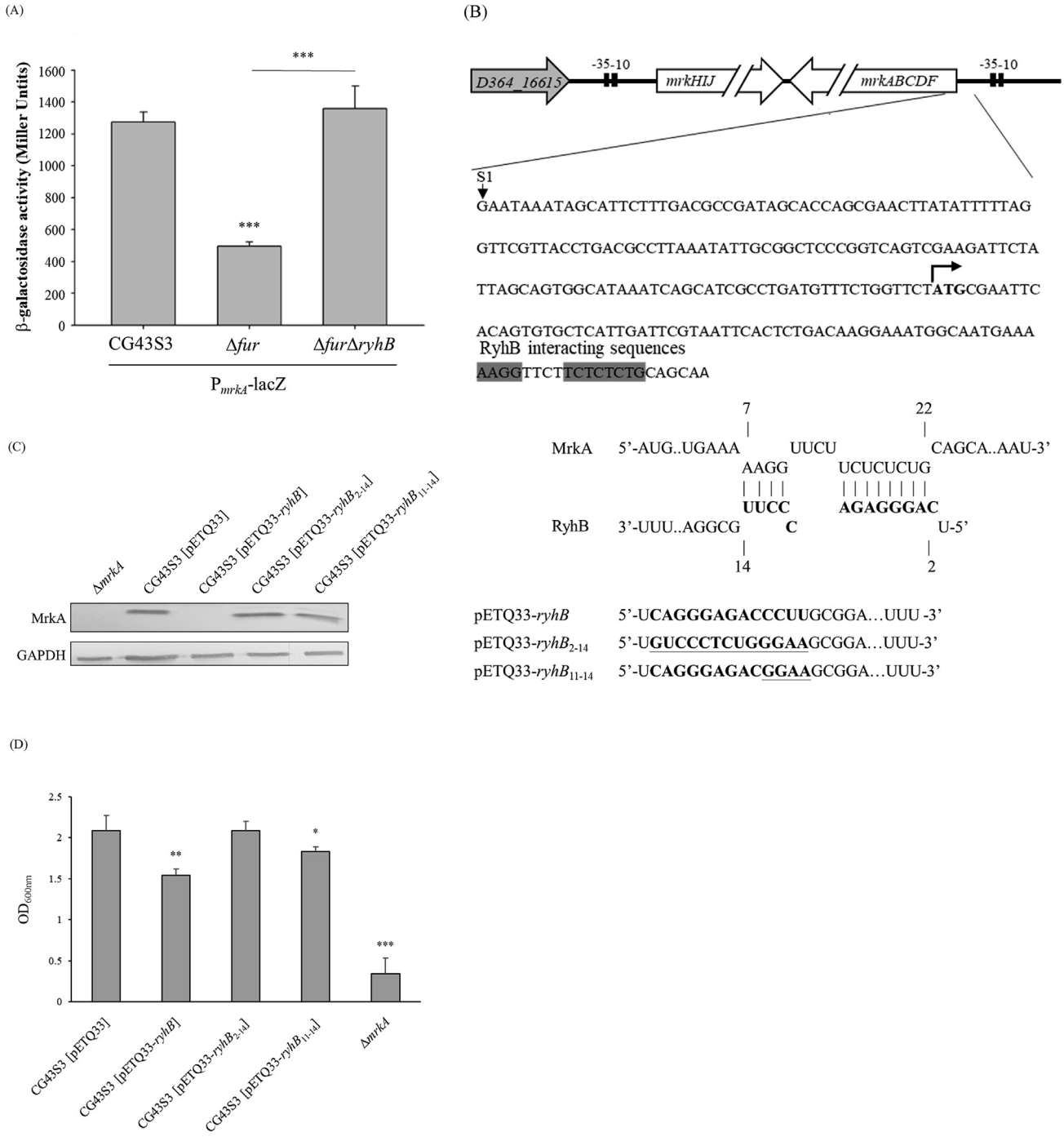

Figure 6. Effect of transforming the recombinant plasmid pETQ-*ryhB*, pET33-*ryhB*$_{2-14}$, or pETQ-*ryhB*$_{11-14}$ into CG43S3 on the expression of type 3 fimbriae. (A) Comparison of the *mrkA* promoter activity in CG43S3, Δ*fur* and Δ*fur*Δ*ryhB* grown in LB broth. The statistical labels indicated that the promoter activity measured in Δ*fur* was significantly different from that in G43S3 and Δ*fur*Δ*ryhB*. (B) Analysis of the putative RyhB-binding sequence on *mrkA* mRNA using intaRNA software (http://rna.informatik.uni-freiburg.de/). Effects of increasing expression of-RyhB, RyhB$_{2-14}$, or RyhB$_{11-14}$ on the production of MrkA (C) and the biofilm formation (D) were analyzed. The statistical labels indicated that the biofilm formation was significantly different from that of CG43S3 [pETQ33].

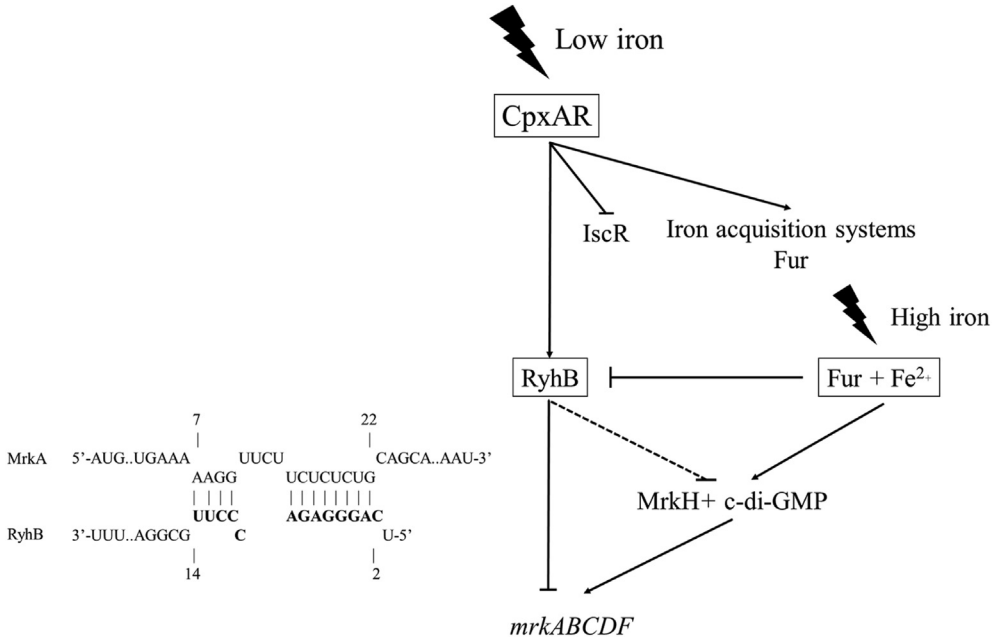

Figure 7. Model of CpxAR-RyhB dependent regulation on the expression of type 3 fimbriae. CpxAR plays a regulatory role in modulating the cellular iron levels through influencing the expression of the iron acquisition system and iron homeostasis regulators Fur, IscR, and RyhB. Under sufficient iron levels, Fur forms a complex with the ferrous ion to activate the expression of *mrkHI* thereafter enhances the expression of type 3 fimbriae. When the cellular iron is lowered to certain levels, the small RNA RyhB, which is no longer repressed by Fur-Fe^{2+}, is activated and concurrently increased expression by CpxAR. The active RyhB directly inhibits the expression of *mrkABCDF* operon that coding for type 3 fimbriae biosynthesis system via base-pairing binding to 5′ sequences of *mrkA* mRNA.

Funding

This study was supported by the grants from Ministry of Science and Technology (MOST 107-2320-B-009-001-MY3) and Center for Intelligent Drug Systems and Smart Bio-devices (IDS2B), National Yang Ming Chiao Tung University, Hsinchu, Taiwan.

Authors' contributions

Conceived and designed the experiments: Chih-Hao Kuo, Wei-Feng Lin, and Hwei-Ling Peng. Performed the experiments: Chih-Hao Kuo, Wei-Feng Lin, Chia-Jui Liu, Zhe-Chong Wang, and Ting-Yi Liu. Analyzed and interpreted the data: Chih-Hao Kuo, Wei-Feng Lin, and Hwei-Ling Peng. Wrote the paper: Chih-Hao Kuo, and Hwei-Ling Peng. All authors read and approved the final manuscript.

Declaration of competing interest

The authors declare that the research was conducted in the absence of any commercial or financial relationships that could be construed as a potential conflict of interest.

Acknowledgments

The authors would like to thank Dr. Ching-Ting Lin of the China Medical University for providing the plasmid pETQ-*ryhB* and anti-Fur antibody. This work was financially supported by the "Center for Intelligent Drug Systems and Smart Bio-devices (IDS2B)" from The Featured Areas Research Center Program within the framework of the Higher Education Sprout Project by the Ministry of Education (MOE) in Taiwan.

References

1. Shon AS, Bajwa RP, Russo TA. Hypervirulent (hypermucoviscous) *Klebsiella pneumoniae*: a new and dangerous breed. *Virulence* 2013;**4**(2):107—18.
2. Martin RM, Bachman MA. Colonization, infection, and the accessory genome of *Klebsiella pneumoniae*. *Front Cell Infect Microbiol* 2018;**8**:4.
3. Paczosa MK, Mecsas J. *Klebsiella pneumoniae*: going on the offense with a strong defense. *Microbiol Mol Biol Rev* 2016; **80**(3):629—61.
4. Tang HL, Chiang MK, Liou WJ, Chen YT, Peng HL, Chiou CS, et al. Correlation between *Klebsiella pneumoniae* carrying pLVPK-derived loci and abscess formation. *Eur J Clin Microbiol Infect Dis* 2010;**29**(6):689—98.
5. Lai YC, Peng HL, Chang HY. RmpA2, an activator of capsule biosynthesis in *Klebsiella pneumoniae* CG43, regulates K2 *cps* gene expression at the transcriptional level. *J Bacteriol* 2003; **185**(3):788—800.
6. Murphy CN, Mortensen MS, Krogfelt KA, Clegg S. Role of *Klebsiella pneumoniae* type 1 and type 3 fimbriae in colonizing silicone tubes implanted into the bladders of mice as a model of catheter-associated urinary tract infections. *Infect Immun* 2013;**81**(8):3009—17.
7. Lin CT, Huang TY, Liang WC, Peng HL. Homologous response regulators KvgA, KvhA and KvhR regulate the synthesis of

capsular polysaccharide in *Klebsiella pneumoniae* CG43 in a coordinated manner. *J Biochem* 2006;**140**(3):429—38.
8. Liu CJ, Lin CT, Chiang JD, Lin CY, Tay YX, Fan LC, et al. RcsB regulation of the YfdX-mediated acid stress response in *Klebsiella pneumoniae* CG43S3. *PLoS One* 2019;**14**(2):e0212909.
9. Cheng HY, Chen YF, Peng HL. Molecular characterization of the PhoPQ-PmrD-PmrAB mediated pathway regulating polymyxin B resistance in *Klebsiella pneumoniae* CG43. *J Biomed Sci* 2010;**17**(1):60.
10. Li H, Liu F, Peng W, Yan K, Zhao H, Liu T, et al. The CpxA/CpxR two-component system affects biofilm formation and virulence in *Actinobacillus pleuropneumoniae*. *Front Cell Infect Microbiol* 2018;**8**:72.
11. Wang ZC, Liu CJ, Huang YJ, Wang YS, Peng HL. PecS regulates the urate-responsive expression of type 1 fimbriae in *Klebsiella pneumoniae* CG43. *Microbiology* 2015;**161**(12):2395—409.
12. Raivio TL, Leblanc SK, Price NL. The *Escherichia coli* Cpx envelope stress response regulates genes of diverse function that impact antibiotic resistance and membrane integrity. *J Bacteriol* 2013;**195**(12):2755—67.
13. Wolfe AJ, Parikh N, Lima BP, Zemaitaitis B. Signal integration by the two-component signal transduction response regulator CpxR. *J Bacteriol* 2008;**190**(7):2314—22.
14. Thanikkal EJ, Gahlot DK, Liu J, Fredriksson Sundbom M, Gurung JM, Ruuth K, et al. The *Yersinia* pseudotuberculosis Cpx envelope stress system contributes to transcriptional activation of *rovM*. *Virulence* 2019;**10**(1):37—57.
15. Subramaniam S, Müller VS, Hering NA, Mollenkopf H, Becker D, Heroven AK, et al. Contribution of the Cpx envelope stress system to metabolism and virulence regulation in *Salmonella enterica* serovar Typhimurium. *PLoS One* 2019;**14**(2):e0211584.
16. Hunke S, Keller R, Müller VS. Signal integration by the Cpx-envelope stress system. *FEMS Microbiol Lett* 2012;**326**(1):12—22.
17. Vogt SL, Raivio TL. Just scratching the surface: an expanding view of the Cpx envelope stress response. *FEMS Microbiol Lett* 2012;**326**(1):2—11.
18. Acosta N, Pukatzki S, Raivio TL. The *Vibrio cholerae* Cpx envelope stress response senses and mediates adaptation to low iron. *J Bacteriol* 2015;**197**(2):262—76.
19. Batchelor E, Walthers D, Kenney LJ, Goulian M. The *Escherichia coli* CpxA-CpxR envelope stress response system regulates expression of the porins *ompF* and *ompC*. *J Bacteriol* 2005;**187**(16):5723—31.
20. Hung DL, Raivio TL, Jones CH, Silhavy TJ, Hultgren SJ. Cpx signaling pathway monitors biogenesis and affects assembly and expression of P pili. *EMBO J* 2001;**20**(7):1508—18.
21. Nevesinjac AZ, Raivio TL. The Cpx envelope stress response affects expression of the type IV bundle-forming pili of enteropathogenic *Escherichia coli*. *J Bacteriol* 2005;**187**(2):672—86.
22. Jagnow J, Clegg S. *Klebsiella pneumoniae* MrkD-mediated biofilm formation on extracellular matrix- and collagen-coated surfaces. *Microbiology (Read)* 2003;**149**(Pt 9):2397—405.
23. Wu CC, Lin CT, Cheng WY, Huang CJ, Wang ZC, Peng HL. Fur-dependent MrkHI regulation of type 3 fimbriae in *Klebsiella pneumoniae* CG43. *Microbiology (Read)* 2012;**158**(Pt 4):1045—56.
24. Skorupski K, Taylor RK. Positive selection vectors for allelic exchange. *Gene* 1996;**169**(1):47—52.
25. Huang SH, Wang CK, Peng HL, Wu CC, Chen YT, Hong YM, et al. Role of the small RNA RyhB in the Fur regulon in mediating the capsular polysaccharide biosynthesis and iron acquisition systems in *Klebsiella pneumoniae*. *BMC Microbiol* 2012;**12**:148.
26. Davis BM, Quinones M, Pratt J, Ding Y, Waldor MK. Characterization of the small untranslated RNA RyhB and its regulon in *Vibrio cholerae*. *J Bacteriol* 2005;**187**(12):4005—14.
27. Massé E, Vanderpool CK, Gottesman S. Effect of RyhB small RNA on global iron use in *Escherichia coli*. *J Bacteriol* 2005;**187**(20):6962—71.
28. Kim JN, Kwon YM. Genetic and phenotypic characterization of the RyhB regulon in *Salmonella* Typhimurium. *Microbiol Res* 2013;**168**(1):41—9.
29. Chareyre S, Mandin P. Bacterial iron homeostasis regulation by sRNAs. *Microbiol Spectr* 2018;**6**(2).
30. Srinivasan VB, Rajamohan G. KpnEF, a new member of the *Klebsiella pneumoniae* cell envelope stress response regulon, is an SMR-type efflux pump involved in broad-spectrum antimicrobial resistance. *Antimicrob Agents Chemother* 2013;**57**(9):4449—62.
31. Srinivasan VB, Vaidyanathan V, Mondal A, Rajamohan G. Role of the two component signal transduction system CpxAR in conferring cefepime and chloramphenicol resistance in *Klebsiella pneumoniae* NTUH-K2044. *PLoS One* 2012;**7**(4):e33777.
32. Cheng HY, Chen YS, Wu CY, Chang HY, Lai YC, Peng HL. RmpA regulation of capsular polysaccharide biosynthesis in *Klebsiella pneumoniae* CG43. *J Bacteriol* 2010;**192**(12):3144—58.
33. Goncalves Mdos S, Delattre C, Balestrino D, Charbonnel N, Elboutachfaiti R, Wadouachi A, et al. Anti-biofilm activity: a function of *Klebsiella pneumoniae* capsular polysaccharide. *PLoS One* 2014;**9**(6):e99995.
34. Kurabayashi K, Hirakawa Y, Tanimoto K, Tomita H, Hirakawa H. Role of the CpxAR two-component signal transduction system in control of fosfomycin resistance and carbon substrate uptake. *J Bacteriol* 2014;**196**(2):248—56.
35. Mey AR, Craig SA, Payne SM. Characterization of *Vibrio cholerae* RyhB: the RyhB regulon and role of *ryhB* in biofilm formation. *Infect Immun* 2005;**73**(9):5706—19.
36. Murphy ER, Payne SM. RyhB, an iron-responsive small RNA molecule, regulates *Shigella dysenteriae* virulence. *Infect Immun* 2007;**75**(7):3470—7.
37. Hernday AD, Braaten BA, Broitman-Maduro G, Engelberts P, Low DA. Regulation of the pap epigenetic switch by CpxAR: phosphorylated CpxR inhibits transition to the phase ON state by competition with Lrp. *Mol Cell* 2004;**16**(4):537—47.
39. Wang ZC, Huang CJ, Huang YJ, Wu CC, Peng HL. FimK regulation on the expression of type 1 fimbriae in *Klebsiella pneumoniae* CG43S3. *Microbiology (Read)* 2013;**159**(Pt 7):1402—15.

Appendix A. Supplementary data

Supplementary data to this article can be found online at https://doi.org/10.1016/j.jmii.2023.02.003.